Flux Creep in Hard Superconductors

Y. B. KIM, C. F. HEMPSTEAD, AND A. R. STRNAD
Bell Telephone Laboratories, Murray Hill, New Jersey
(Received 7 May 1963)

Resistive states of hard superconductors have been investigated by tube magnetization and resistance measurements. The flux-creep theory of Anderson is very effective in accounting for the experimental observations reported herein. Resistive phenomena were observed in the presence of transport current density J and magnetic field B perpendicular to J. It is found that the whole spectrum of resistive states can be represented in terms of a single parameter $\alpha=J(B+B_0)$, where B_0 is a constant of the material. This parameter represents essentially the Lorentz force or the magnetic pressure gradient in the material. While a wide range of α values is possible, under given experimental conditions superconductivity usually can not be maintained above a critical value. In tube magnetization, the critical value α_c is determined primarily by the rate with which the persistent current J decays. If α is raised beyond α_c, J decays rapidly and α quickly falls near to α_c. α continues to decrease slowly, but proportional to the logarithm of time as predicted by the theory. The observed temperature dependence of α_c is accounted for by the theory. Discrete, stochastic changes in field anticipated from the motion of flux bundles have been detected through pickup coils placed in close proximity to the superconducting tube. In resistance measurements, voltages appearing across 3Nb-Zr wire samples were measured by supplying J externally in the presence of a perpendicular field H. The voltage observed is interpreted as a manifestation of an uncompensated emf arising from flux creep. At a given temperature, voltage readings obtained over a wide range of J and H are found to be a function of $\alpha=J(H+B_0)$ only. $V(\alpha,T)$ follows qualitatively a form expected from the theory. In resistance measurements, the critical value α_p is determined by the power dissipation in the material. If α is raised beyond α_p, thermal conduction lags the power dissipation and the sample undergoes a catastrophic transition to the normal state.

I. INTRODUCTION

RECENTLY, we have reported[1,2] that in bulk hard superconductors the critical current density J in the presence of transverse magnetic field B is limited by the Lorentz force parameter $\alpha\sim JB<\alpha_c$. α_c is a structure-sensitive constant of the material and its dependence on temperature is nearly linear as far down as $0.1T_c$, where none of the bulk superconducting properties is expected to vary noticeably. To account for these observations, Anderson[3] introduced a mechanism of flux creep arising from thermal activation. In consequence, his theory predicts the decay of persistent currents proportional to the logarithm of time. This logarithmic decay has been observed[1] from one to about 10^4 sec. In this article we report additional experimental facts that can be explained most naturally by the flux-creep model. In particular, it will be shown that the broad resistive transitions commonly observed in hard superconductors can be represented in terms of the Lorentz force parameter α.

Insofar as the bulk electromagnetic properties are concerned, superconductors may be classified into three groups. The phenomenological theory of London[4] is very effective in accounting for the properties of ideal soft superconductors, or *S*I. The possible existence of another group of superconductors *S*II has been indicated by the theory of Ginzburg and Landau,[5] which has been shown to follow from the microscopic theory of BCS[6] by Gor'kov.[7] According to the theoretical work by Abrikosov,[8] and later by Goodman,[9] a bulk sample of homogeneous, strain-free *S*II material enters into a mixed state in a region of magnetic fields $H_{c1}<H_c<H_{c2}$, below and above the thermodynamic critical field H_c. Essential to the occurrence of the mixed state is a small coherence distance in the superconducting state, since this leads to a negative interphase surface energy and makes the mixed state thermodynamically stable. Thus, the magnetic behavior in the mixed state is expected to be reversible and independent of the sample size. Many recent experiments[10] support the existence of a mixed state when the sample is made homogeneous and strain-free. *S*II materials in the mixed state allow the flow of body currents because of the field penetration in the form of flux filaments, but they are not expected to support large transport current densities. In the presence of transport currents transverse to the magnetic field, the Lorentz force will set either the flux filaments or the superconducting regions into a continual lateral motion,[11] thereby developing an effective resistance in

[1] Y. B. Kim, C. F. Hempstead, and A. R. Strnad, Phys. Rev. Letters **9**, 306 (1962).
[2] Y. B. Kim, C. F. Hempstead, and A. R. Strnad, Phys. Rev. **129**, 528 (1963).
[3] P. W. Anderson, Phys. Rev. Letters **9**, 309 (1962).
[4] F. London, *Superfluids* (Dover Publications, Inc., New York, 1960), Vol. 1.
[5] V. L. Ginzburg and L. D. Landau, Zh. Eksperim. i Teor. Fiz. **20**, 1064 (1950).
[6] J. Bardeen, L. N. Cooper, and T. R. Schrieffer, Phys. Rev. **108**, 1175 (1957).
[7] L. P. Gor'kov, Zh. Eksperim. i Teor. Fiz. **36**, 1918 (1959); **37**, 833 (1959) [translations: Soviet Phys.—JETP **9**, 1364 (1959); **10**, 593 (1960)].
[8] A. A. Abrikosov, Zh. Eksperim. i Teor. Fiz. **32**, 1442 (1957) [translation: Soviet Phys.—JETP **5**, 1174 (1957)].
[9] B. B. Goodman, Phys. Rev. Letters **6**, 597 (1961).
[10] Abrikosov mixed-state behavior has been observed in Ta-Nb by A. Calverley and A. C. Rose-Innes, Proc. Roy. Soc. (London) **A255**, 267 (1960); in Nb by T. F. Stromberg and C. A. Swenson, Phys. Rev. Letters **9**, 370 (1962); in In-Bi by T. Kinsel, E. A. Lynton, and B. Serin, Phys. Letters **3**, 30 (1962); and in Mo-Re by J. K. Hulm, 8th Conference on Magnetism and Magnetic Materials, Pittsburgh, Pennsylvania, (unpublished).
[11] J. C. Gorter, Phys. Letters **1**, 69 (1962); **2**, 26 (1962).

the material. Thus, in the high-field superconducting materials capable of supporting large transport current densities, some mechanism must be present to provide a rigidity against the Lorentz force. These materials are basically of the *S*II type, but contain a large amount of structural irregularities such as impurities, strains, dislocations, or other physical defects. In this respect, we may call these materials the third group, or *S*III. If structural irregularities are introduced in *S*I materials, in many respects they also behave like *S*III.

In Anderson's flux-creep theory,[3] the moving entities are assumed to be the bundles of magnetic flux which may contain single or many quantized flux filaments. Although the internal structure of a flux bundle is visualized as similar to the Abrikosov structure,[8] the theory does not take this into account explicitly. Structural irregularities present in an *S*III material are assumed to pin down flux bundles and act as free-energy barriers. A flux bundle so pinned, however, can hop the barrier by thermal activation aided by the Lorentz force. This concept of activated motion of flux structures and a simple theory resulting from this concept are substantiated by the experimental facts reported below.

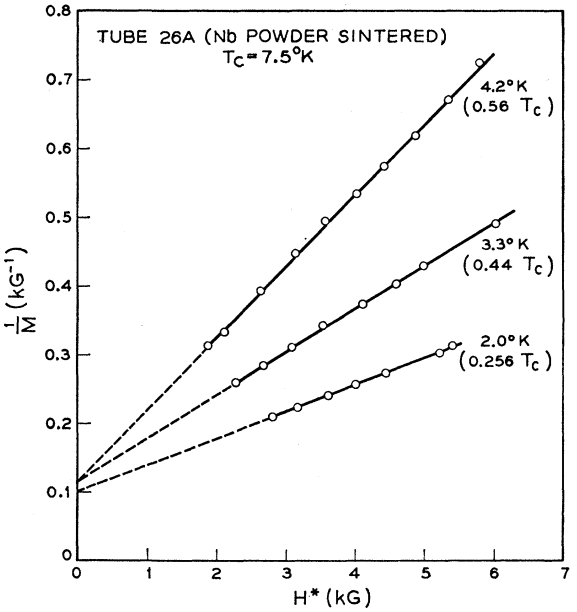

FIG. 2. $1/M$ versus H^* plots for a Nb powder sintered tube. $H'(H)$ curves for this tube at 4.2 and 3.3°K are given in Fig. 1 of Ref. 1.

II. TUBE MAGNETIZATION AND FLUX CREEP

Inasmuch as Anderson's flux-creep theory was developed in parallel with our tube magnetization experiments, we will first summarize the analytical approach used in tube experiments and its connections to the flux-creep theory. If the external field H, applied parallel to the axis of a hard superconducting tube, is varied, the axial field H' inside the tube follows along a curve[12] such as shown in Fig. 1. When the values of H and H' lie on this curve, the sample is said to be in a critical state, wherein every macroscopic region of the sample is assumed to carry the critical current density $J(B)$ determined only by the local magnetic field B at that region. Once $J(B)$ is specified, H' in a critical state is determined from the relation

$$H'=H+4\pi\int_0^w J[B(r)]dr, \tag{1}$$

where r is a radical variable measured inward from the outer surface of the tube. Elimination of r leads to an integral relation

$$4\pi w=\int_{H^*-\frac{1}{2}M}^{H^*+\frac{1}{2}M}\frac{dB}{J(B)}, \tag{2}$$

where $H^*=\frac{1}{2}(H'+H)$ is the mean field in the sample wall, and $M=H'-H$ is the field produced by the induced supercurrent. The average current density in the wall is then given by $M/4\pi w$. Since H^*, M, and w are available from experiments, (2) enables us to deduce $J(B)$ empirically.

For many *S*III materials, the critical-state curve $H'(H)$ consists of two hyperbolas and one circle. A more sensitive way of representing such systematics is to plot the data points in the $1/M-H^*$ plane. A typical

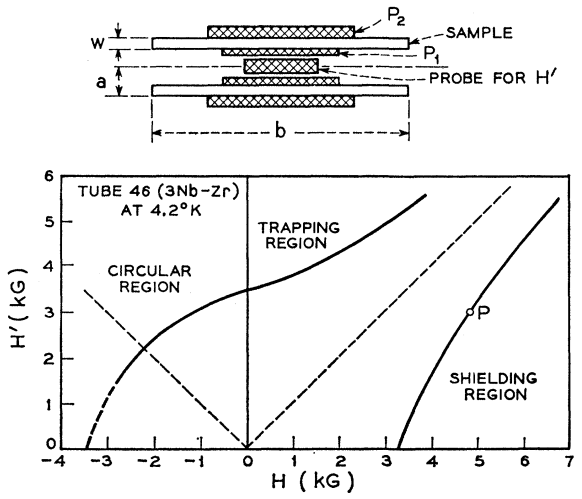

FIG. 1. Tube magnetization curve of a 3Nb-Zr tube. $\alpha_c=5.0\times10^6$ emu (G-abamp/cm^2) and $B_0=1.1$ kG are obtained from this magnetization curve. P is the point at which a 3-h decay run was made with a YIG probe. The insert shows the tube geometry ($a=0.33$ cm, $w=0.153$ cm, $b=4.45$ cm) and the pickup coil arrangement used for pulse detection. Pulses observed in P_1 and P_2 are shown in Fig. 5.

[12] If H is changed too fast, a flux jump occurs and H' falls quickly to H. The flux jump is more frequent in the low-field–high-current region and is believed to be caused by locally excessive values of α.

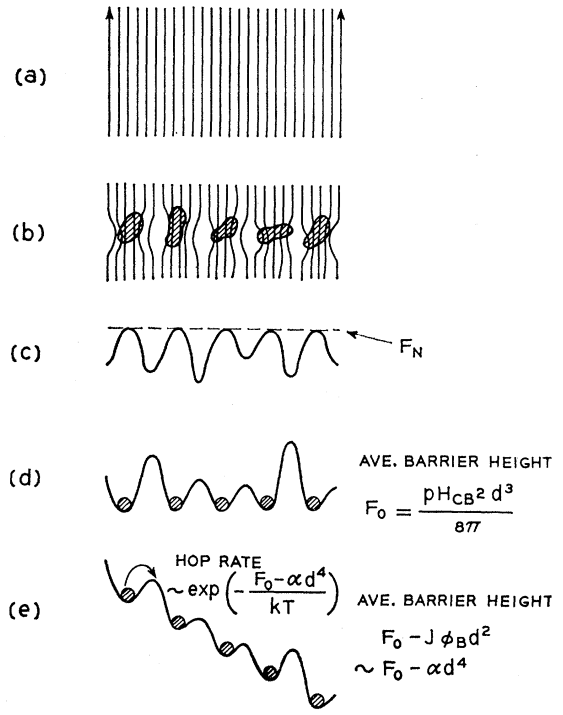

FIG. 3. A schematic model of flux creep.

plot of $1/M$ versus H^* obtained with a Nb powder sintered tube is shown in Fig. 2. Representing the straight line by

$$4\pi w\alpha_c/M = B_0 + H^*, \tag{3}$$

two constants α_c and B_0 can be obtained from the slope and the intercept. The critical-state curve $H'(H)$ associated with this straight line is given by two hyperbolas

$$(H'+B_0)^2-(H+B_0)^2=\pm 8\pi w\alpha_c, \tag{4}$$

and a circle

$$(H'+B_0)^2+(H-B_0)^2=2(4\pi w\alpha_c+B_0^2). \tag{5}$$

It is now readily seen that (3) follows from (2) for a critical current density relation

$$\alpha = J(B+B_0)=\alpha_c. \tag{6}$$

Note that for $B \gg B_0$, the parameter

$$\alpha \sim JB = |(H'^2-H^2)/8\pi w| \tag{7}$$

represents the Lorentz force or the magnetic pressure gradient in the sample. Thus, the supercurrent density in an *S*III material cannot be raised beyond the point where the Lorentz force parameter α exceeds a certain critical value α_c.

The values of α_c are generally larger for *S*III materials having higher transition temperature T_c. For a material of given chemical composition, however, α_c is strongly influenced by the amount of structural irregularities in the material, although the presence of such irregularities does not affect T_c. Also, α_c depends strongly on temperature, even down to a low-temperature range where none of the bulk superconducting properties is expected to vary noticeably. This is apparent from Fig. 2. As T is lowered, α_c (the inverse of slope) increases linearly in T. This trend is common to *S*III materials investigated in our tube experiments (Nb powder sintered material, Nb-Zr alloys, Nb_3Sn intermetallic compounds), and an empirical relation,

$$(F_0-q\alpha_c)/kT = \text{const}, \tag{8}$$

has been established. The significance of F_0 and q will become apparent from the flux-creep theory.

Anderson[3] inferred a thermally activated process from the empirical relation (8), and developed a simple theory which is quite effective in accounting for the transport current properties of *S*III materials. The working model behind this theory is shown schematically in Fig. 3. (a) represents the periodic structure of flux lines in the Abrikosov mixed state. When the separation between flux lines becomes of the order of London penetration depth $\lambda_L \sim 5\times 10^{-6}$ cm, flux lines will be bound together to some extent by the interaction of their fields and wave functions. Physical irregularities present in an *S*III material may also aid the formation of such flux "bundles" as in (b). (c) shows the spatial variation in free energy for such a structure. Since the physical irregularities tend to pin down the flux bundles, free-energy maxima centered around these irregularities will become free-energy minima for the motion of flux bundles (d). The average energy barrier experienced by the bundles is then expressed by

$$F_0 = pH_{cB}^2 d^3/8\pi, \tag{9}$$

where H_{cB} is the bulk critical field and p is a parameter representing the pinning strength. In the presence of transport current density J (transverse to B), the Lorentz force JB on flux bundles will result in a tilting of the barrier structure as in (e). This, in effect, reduces the barrier height to

$$F_0 - J\varphi_B d^2 = F_0 - \alpha d^4, \tag{10}$$

where $\varphi_B = Bd^2$ is the total flux in the bundle. The inter-bundle spacing, as well as the length of the bundle which can move independently, are assumed to be of the order of d. For other possibilities, the d^4 factor will contain additional parameters. The approximation $\alpha \sim JB$ holds only in the high-field limit where $B \gg B_0$. Thermal activation now enables the bundle to hop a barrier and go down the hill. This rate is given by

$$\text{Hop rate} = R_0 \exp[-(F_0-q\alpha)/kT], \tag{11}$$

where R_0 is an appropriate frequency factor. We have replaced the d^4 factor by q, anticipating various modifications to the theory.

In the tube experiment, if H is held at a constant value greater than H', the flux bundles creep into the tube and the difference $|M|=H-H'$ will become smaller in time, that is, the persistent currents decay. This consideration leads to an equation of creep rate

$$\frac{d}{dt}(H-H')=-\frac{2dR_0H^*}{ca}\exp\left[\frac{-(F_0-q\alpha)}{kT}\right], \quad (12)$$

where c is a parameter giving the number of effective barriers that are encountered by a bundle in crossing the tube wall. According to this theory, the critical state as observed in tube experiments represents only a quasiequilibrium state at which the rate falls below a practically observable limit. Under this condition, the exponent in (12) will become a constant and α therein will be identified experimentally as α_c, leading to the empirical relation (8). The observed linearity of α_c with T follows simply from the fact that F_0 is insensitive to temperature at low temperatures.

Since the creep in (12) continues at any values of J and B, the value of α in the sample will be continually decreasing. The theory is specific on this time behavior of α and predicts

$$\delta\alpha=\text{const}-(kT/q)\ln t. \quad (13)$$

In terms of the observable quantity H', (13) gives

$$\delta H'=-\frac{4\pi w}{H'+B_0}\frac{kT}{q}\ln t. \quad (14)$$

In other words, the internal field H' will change logarithmically in time. Experimental verifications of this logarithmic behavior have been reported earlier.[1] In recent runs, we have been using a sensitive yttrium iron garnet (YIG) electron spin resonance probe to measure H' with a precision of one part in 10^5. All runs made with this YIG probe verify the logarithmic decay to a high degree of accuracy. For example, a decay run made at P of Fig. 1, which lasted for 10^4 sec, gave $dH'/d(\ln t)=(5.01\pm0.02)$ G per decade. The dependence of decay rates on field and temperature are currently being investigated with the YIG probe.

So far, we have described a particular group of *S*III materials for which the Lorentz force relation (6) holds almost up to the upper critical field. For classification purposes, we may call them *ideal* *S*III's. Two samples shown in Fig. 4 do not behave in this way. In the Nb metal tube, if the lower shielding portion of $H'(H)$ is fitted to (6), the critical current density at high fields is much lower than that expected from (6). In the V metal tube, the situation is reversed in that the critical current density at low fields is too small. In spite of such deviations, however, we do observe logarithmic changes in H' for both Nb and V tubes. The logarithmic decay has also been observed near the upper critical field of ideal *S*III samples, where $H'(H)$ no longer follows from (6). DeFeo and Sacerdoti[13] observed the trapped flux in a Pb ring to decay under the bombardment of α particles. Replotting their data, we find this decay is also logarithmic up to $t\sim1.5\times10^5$ sec, the period of their observations. Thus, the logarithmic decay process appears to be quite general in a certain domain of superconductivity.

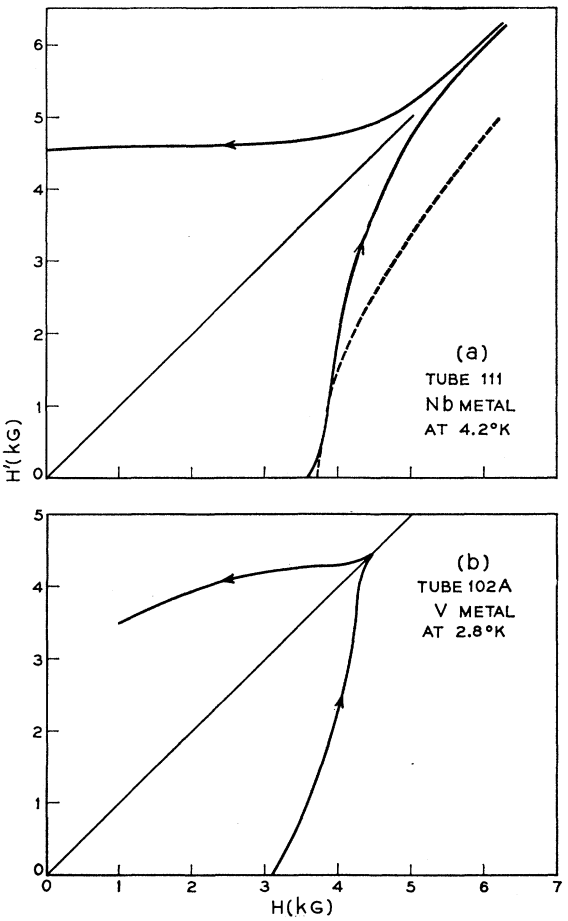

FIG. 4. Tube magnetization curves for (a) a Nb metal tube, (b) a V metal tube. The dashed line in (a) is obtained by fitting the lower portion of the observed curve to expression (6) of the text.

III. MOTION OF FLUX BUNDLES

According to the flux-creep model, the motion of flux bundles is expected to be discrete and stochastic. Anticipating that this behavior would be reflected in the change of magnetic fields, we placed pickup coils inside (P_1) and outside (P_2) the 3Nb-Zr tube shown in Fig. 1. Signals in the pickup coils were displayed on an oscilloscope via a low noise amplifier having a voltage gain of about 900. Typical pulse signals observed in P_1 at the shielding portion of $H'(H)$ are shown in Fig. 5a. Signals

[13] P. DeFeo and G. Sacerdoti, Phys. Letters 2, 264 (1962). The fact that the trapped flux decay observed by these authors follows a logarithmic decay law was pointed out by P. W. Anderson.

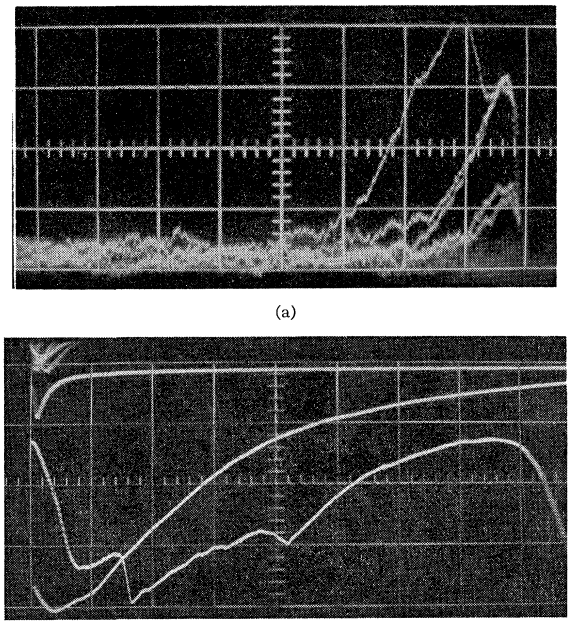

(a)

(b)

FIG. 5. Pulses observed in pickup coils of Fig. 1: (a) pulses observed in P_1 at the shielding region (20 μsec/div, 5μV/div); (b) pulses observed in P_2 at the circular region (200 μsec/div, 2 mV/div).

vary in amplitude, but they all have about the same rise time. Calibrations of the pickup coil and amplifier system indicate that such a signal results from a voltage pulse lasting for about 10 μsec or less, and the signal amplitude is proportional to the voltage impulse $\int V dt$. The smallest signals discernable from noise are estimated to contain 20 to 50 flux quanta.

In the shielding region of $H'(H)$, where $H'<H$ and flux creeps inward, we observe unidirectional pulses in P_1 but not P_2. In the trapping portion where flux creep outward, we observe similar pulses in P_2 but not P_1. It appears that flux leaves the tube in the form of bundles, but flux replenishment from the other side of the tube need not be in the form of bundles, or the bundles are too small to be detected. Pulses are frequent near the critical state where flux creeps faster. If H is held at a constant value on $H'(H)$, the number of pulses decreases in time in a manner consistent with the logarithmic decay in H'. In the circular region, pulses in P_2 are dominated by the type shown in Fig. 5b. Such pulses are also observed occasionally in P_1. These large, wide pulses, or a succession of them, may be due to an avalanche motion of flux bundles or/and some sort of domain motion.[14] Pulses qualitatively similar to those shown in Fig. 5a, but much smaller in amplitude, have also been observed in a Nb_3Sn tube. Although a quantitative interpretation requires further work, the basic concept of activated motion of flux structures seems very real in these pulse observations.

IV. RESISTANCE DUE TO FLUX CREEP

Energy dissipation associated with flux creep is quite different from ordinary ohmic dissipation. Nevertheless, we may associate an equivalent electrical resistance with the flux creep by a simple argument. Since $H-H'=4\pi I/b$ (see Fig. 1), the change in H' due to flux creep is interpreted as a decay of persistent current I in the tube wall, with a rate

$$dI/dt=(b/4\pi)(d/dt)(H-H'). \tag{15}$$

For the closed system, we may attribute this change in I to an equivalent R by the circuit equation

$$L(dI/dt)+RI=0. \tag{16}$$

Taking the case $w\ll a\ll b$, which leads to $L\simeq 4\pi^2a^2/b$ and $R\simeq\rho 2\pi a/(bw)$, we derive an expression for the resistivity,

$$\rho=2\pi aw\left|\frac{1}{I}\frac{dI}{dt}\right|=2\pi aw\left|\frac{1}{H-H'}\frac{dH'}{dt}\right|. \tag{17}$$

At P of Fig. 1, using the above expression, we estimate $\rho=3\times10^{-13}$ Ω-cm at the very beginning of the decay run. As the current decays due to flux creep, ρ falls as $1/t$. After 10^4 sec, ρ then falls to 3×10^{-17} Ω-cm. In spite of this large change in ρ, however, α decreases by only 1% during this period.

In our tube experiments, the test of logarithmic decay is confined to a very small range of α near α_c. For α substantially smaller than α_c, the experiment is difficult because of the enormously long time scale involved.[15] For $\alpha>\alpha_c$, on the other hand, the decay is too fast to be measured conveniently. We, therefore, proceeded to test logarithmic decay over a wide range of α values. This amounted to measuring the resistance of a sample by supplying a constant current externally in the presence of a transverse field H. Under this condition, flux creep generates an uncompensated emf and a voltage will appear along the direction of current flow. We expect this voltage to be dominated by the exponential term in (11), i.e.,

$$V=f\exp[-(F_0-q\alpha)/kT]. \tag{18}$$

For a sample of small cross-sectional area, B appearing in α [see (6)] may be approximated by H. The factor f depends on the sample geometry and contains some of the structural constants defined by Anderson.[3] It may also depend on J and H.

To check expression (18), we measured the voltage

[14] Fluctuation of the resistance in *S*III materials, probably due to domain motions, was reported by B. Lalevic, Phys. Rev. **128**, 1070 (1962). Earlier work on domain motions are quoted in this article.

[15] J. File and R. G. Mills, Phys. Rev. Letters **10**, 93 (1963), observed a persistent current decay in a closed Nb-Zr coil at a level of $\rho\sim5\times10^{-22}$ Ω-cm. We feel their observation is consistent with the flux-creep model, although it may be due to some other effects.

across a 3Nb-Zr wire[16] (250 cm long, and 0.0076 cm in diameter), either varying J at constant H or varying H at constant J. For a given set of J and H values, these two methods yielded the same voltage reading within the experimental errors. In Fig. 6 are shown V's as a function of H for different sets of constant J's, all taken at 4.2°K. It is evident that V depends strongly on J and H. If we assign a resistivity to the material by the relation $\rho=V/(lJ)$, where l is the length of the wire, we obtain values as indicated in the figure.[17] As J is decreased, the transition becomes broader. In other words, the resistive state appears over a wider range of H.These

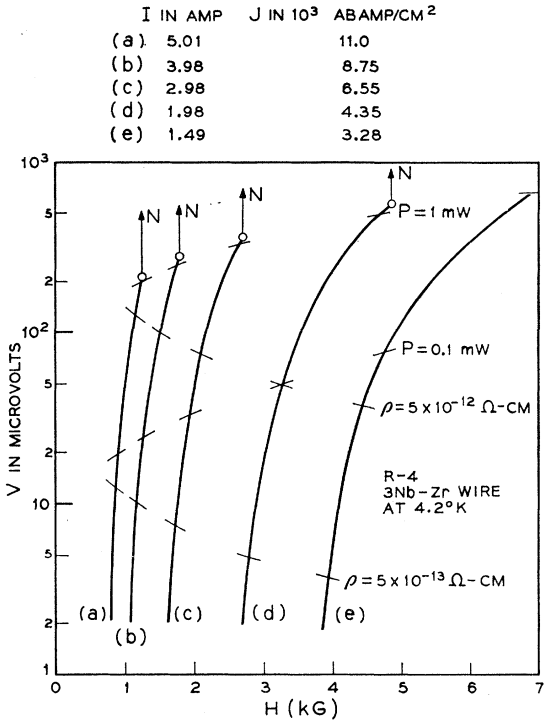

FIG. 6. Voltages observed across a 3Nb-Zr wire (250 cm long). Voltage readings were taken with a digital voltmeter (0.5-μV sensitivity) as a function of H at various current settings. Vertical arrows indicate catastrophic transitions to the normal state. All these transitions took place at $P=VI=1.1$ mW. ρ values shown are calculated from $\rho=V/(lJ)$, where $l=250$ cm. ρ (300°K) $=35\,\mu\Omega$-cm and ρ (77°K) $=26\,\mu\Omega$-cm were obtained for this sample.

characteristics have been commonly observed in earlier work, but no convincing theory has been put forward to explain this behavior.

In order to compare our data with (18), we carried out the following analysis.

[16] Commercially supplied 3Nb-Zr wire was annealed for one hour at 1125°C. Two ends of a wire sample were clamped into large copper blocks which served as lead-in current terminals. Voltage leads were attached to the sample about 3 cm away from the copper blocks.

[17] The resistivity obtained in this way is a gross underestimate. See Sec. V.

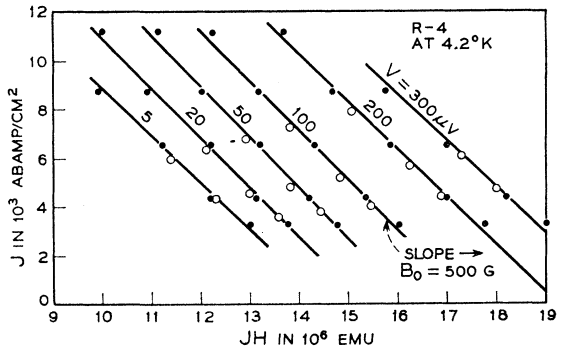

FIG. 7. J versus JH plots for constants V's. The data points obtained from Fig. 6 are shown by the dots. With the same sample, voltage readings were also taken by varying J at constant H's. These data are shown by the circles. The slope of $V=100\,\mu$V line yields $B_0=0.5$ kG.

A. Determination of B_0

From (18) we obtain

$$\ln V=\ln f-\frac{F_0}{kT}+\frac{q}{kT}JH+\frac{q}{kT}B_0J. \qquad (18.1)$$

If f and F_0 are insensitive to J and H, sets of J and H values yielding a constant V should fall on a straight line in the J–JH plane, with a slope of $-1/B_0$. Such a plot obtained from the data of Fig. 6 is shown in Fig. 7. The data obtained by varying J at constant H are also

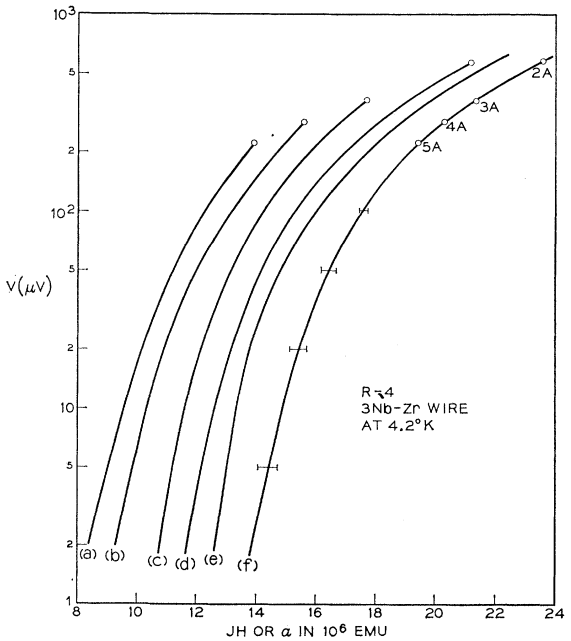

FIG. 8. V as a function of α. Curves of Fig. 6 are first plotted against JH, then against $\alpha=J(H+B_0)$ with $B_0=0.5$ kG as obtained in Fig. 7. In the $V-\alpha$ plot, all curves [(a) to (e)] of Fig. 6 coalesce into a single curve (f), within the limits shown by the horizontal flags. Open circles indicate normal transitions occurring at various current settings.

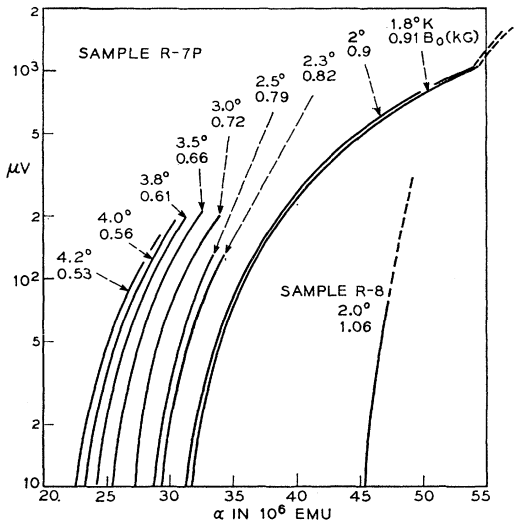

FIG. 9. $V(\alpha)$'s at various T's. At each temperature, B_0 was obtained from a plot similar to Fig. 7. Using B_0 so obtained, $V(H)$ curves at different J's have been reduced into a single curve $V(\alpha)$. Below $T\lambda$, the dashed portions of $V(\alpha)$'s indicate where the sample temperature rose above the bath temperature.

included. From the slope of parallel straight lines, we obtain $B_0=0.5$ kG. What is actually implied by this plot is that at a given temperature V is a function of α only.[18]

B. Dependence of V on α

Having obtained B_0, we can display V directly as a function of $\alpha=J(H+B_0)$. We find then all curves of Fig. 6 coalesce into a single curve, as expected from the analysis in A. This is shown in Fig. 8 in two steps. The curves of Fig. 6 are first plotted against JH to show that they are nearly parallel in this representation. The addition of JB_0 to the abscissa displaces each curve to the right by such an amount as to coalesce all curves to (f). The degree of this coalescence is indicated by the horizontal flags, the scatter being larger in the low voltage range where the measurements are more subject to noise. There are some second-order systematic trends in the scatter which require further investigation. However, the basic dependence of V on J and H can be represented in terms of the single parameter α.

From (18), we can formally derive

$$\frac{\partial \ln V}{\partial \alpha}=\frac{\partial \ln f}{\partial \alpha}-\frac{1}{kT}\frac{\partial F_0}{\partial \alpha}+\frac{q}{kT}. \tag{19}$$

As long as the exponential term in (18) dominates V, and F_0 is insensitive to α, we expect to observe the slope

$$\partial \ln V/\partial \alpha=q/kT \tag{20}$$

to be constant at a given temperature. The experimental curves show, however, that as α or V increases, the slope decreases. At the largest values of V, the slope drops until V is almost linear in α.[19] Neither the probable dependence of F_0 on α nor the possibility of the sample being at a higher temperature than the bath accounts for this behavior. Both of these effects would tend to raise V at large values of α, rather than lowering it. As for the possible dependence of f on α, some estimates can be made using the rate equation (12). For a tubular geometry, the back emf $V=-LdI/dt=RI$ arising from flux creep is determined by (12) and leads to

$$f=2\pi a d R_0 H^*/c. \tag{21}$$

For a wire sample, we estimate

$$f\sim l d R_0 H/c. \tag{22}$$

The approximation $2\pi a\rightarrow l$ (the length of a wire sample) is very crude, but f must depend on H because of dimensional considerations. The present data, however, do not exhibit this particular field dependence of f. Thus, the theory in its present form is inadequate to explain the observed behavior of V in α. The assumption of a constant average barrier height used in the theory can be satisfactory only over a small range of α values, a situation typical of the tube experiments. There must certainly be a distribution in barrier heights and the number of effective barriers will decrease as α increases. Such parameters as F_0, q, and c will change depending on a specific distribution in barrier heights.

C. Temperature Dependence

Figure 9 shows how V depends on α at a number of different temperatures. The curves were obtained from a different 250-cm-long sample of 3Nb-Zr wire. The values of B_0 obtained at each temperature are shown in the figure. B_0 increases as T is lowered, as has also been observed in tube experiments. As T is lowered, a higher α value is required to give the same voltage V. Clearly, as the thermal activity is decreased, a greater tilting of the barrier structure by α is required to give the same flux-creep rate and thus V.

To test the specific temperature dependence pre-

[18] If V depends only on α, then

$$\delta V(\alpha)=\frac{dV}{d\alpha}\delta\alpha=\frac{dV}{d\alpha}\left[\frac{\partial \alpha}{\partial (JH)}+\frac{\partial \alpha}{\partial J}\frac{dJ}{d(JH)}\right]\delta(JH).$$

For $V(\alpha)=$const, i.e., $\delta V=0$, $\delta\alpha=0$ leads to

$$\frac{\partial \alpha}{\partial (JH)}+\frac{\partial \alpha}{\partial J}\frac{dJ}{d(JH)}=1+B_0\frac{dJ}{d(JH)}=0,$$

or $dJ/d(JH)=-1/B_0$ which is observed in Fig. 7.

[19] P. W. Anderson has pointed out that this behavior suggests a viscous flow of flux lines rather than creep. At sufficiently large values of α, a point may be reached at which the average barriers are nearly overcome by the force. At such a point the exponential dependence on α will cease and a new conventional rate equation will become effective, the rate being proportional to force, or α. This is compared to the difference in magnetic domain motion below and above the "coercive force": below; slow, creeplike processes occur, while above one has viscous motion of the domain walls with velocity proportional to H.

dicted by (18), we may rewrite it as

$$\alpha = F_0/q - [(k/q)\ln(f/V)]T, \qquad (18.2)$$

and compare this expression with the observed dependence of α on T at a constant V. In Fig. 10 is plotted a family of data points at various fixed values of V. The linear dependence of α on T as implied by (18.2) is apparent. Although this test is somewhat obscured because of the uncertainties mentioned in (b), it should be noted that (18.2) is essentially the same expression as $\alpha_c(T)$ from the tube experiments [see (8)], but at much higher levels of V. The slope $d\alpha_V/dT \sim 3.5\times10^6$ emu/deg for this wire sample, compared to $d\alpha_c/dT \sim 1.2\times10^6$ emu/deg for the 3Nb-Zr tube of Fig. 1. Discontinuities are present at the helium λ transition temperature T_λ. These could be caused by different thermal conditions above and below T_λ. Further investigation is required to clarify this point.

From the above analysis, it is empirically shown that in 3Nb-Zr wire samples, $V(J,H,T)$ reduces to $V(\alpha,T)$ given by (18), a form expected from the flux-creep theory. Verification of the theory resulting from voltage measurements is essentially of the same quality as that from the tube experiments. The voltage measurements are, however, more explicit in showing that the effect due to a distribution in barrier heights may have to be taken into account in the theory. Friedel, DeGennes, and Matricon[20] have recently made a refined calculation on the driving force in flux-creep phenomena, but have not explicitly included the effect of a distribution in barrier heights.

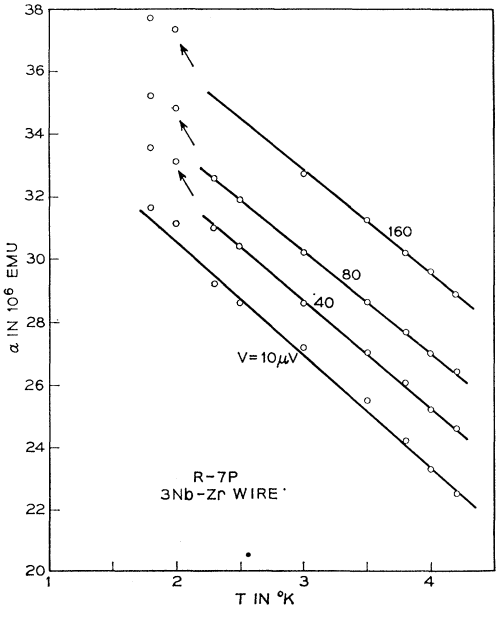

FIG. 10. α versus T at a constant V. At various fixed values of V, the values of α obtained from Fig. 9 are plotted versus T.

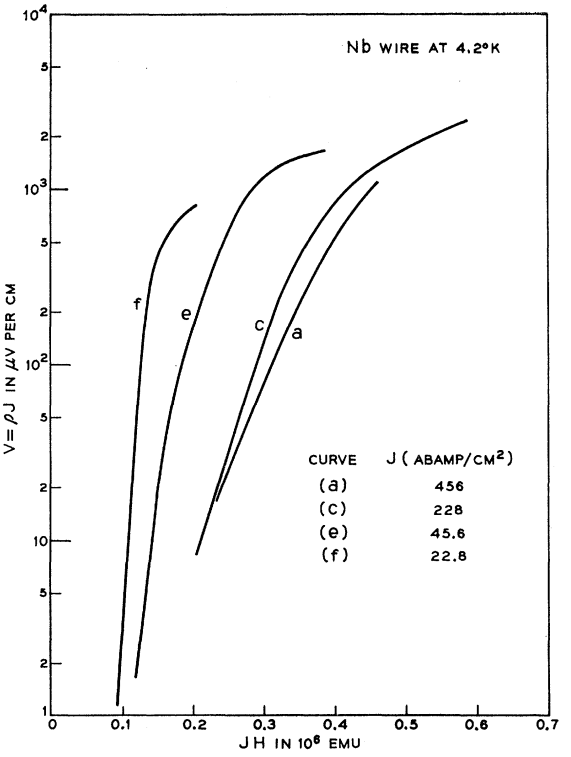

FIG. 11. V versus JH for a Nb wire. Part of Fig. 1 of Ref. 21 is converted into the form V per unit length of the sample versus JH. $V=\rho J=(\rho/\rho_n)J\rho_n$ is calculated from their data with $\rho_n=3.6$ $\mu\Omega$-cm. For curves (e) and (f), the "peak effects," or the dips in resistance, observed at $H=5.5$ kG are not shown. For all curves, the lower ends represent $\rho/\rho_n \sim 10^{-3}$, while the upper ends represent $\rho/\rho_n=0.07$, 0.3, 1.0, and 0.9 for curves (a), (c), (e), and (f), respectively.

We again expect (18) to hold closely only for the class of ideal *S*III materials. As an illustration, we cite the resistance measurements on Nb wires reported by Autler, Rosenblum, and Gooen.[21] In Fig. 11, part of their data are shown in the form of V versus JH. For curves (e) and (f), we ignored the "peak effect" observed by these authors at $H=5.5$ kG. Clearly, there exists no positive constant B_0 that may help these curves to coalesce (see Fig. 8 for comparison). If (18) is fitted, for example, to curve (a), experimental curves for low J at high fields give a higher resistance than expected. In tube experiments, this material would give critical current densities at high fields much lower than that expected from (6). This is what is observed in the Nb tube data shown in Fig. 4(a).

[20] J. Friedel, P. G. DeGennes, and J. Matricon, Appl. Phys. Letters **2**, 119 (1963).

[21] S. H. Autler, E. S. Rosenblum, and K. H. Gooen, Phys. Rev. Letters **9**, 489 (1962). We are indebted to Dr. S. H. Autler for the detailed experimental data used in our comparison.

V. POWER DISSIPATION

When a superconducting sample is driven into a resistive state, power is dissipated in the material. The power dissipation per unit volume may be expressed as

$$P=VJ/l=(f/l)J\exp[-(F_0-q\alpha)/kT], \quad (23)$$

where l is the length of that part of the sample across which the voltage appears. This power may be small, but its extreme temperature dependence must be considered. Thermal equilibrium is possible only when a proper balance is maintained between the power dissipation and thermal conduction to the bath. Once thermal conduction begins to lag power dissipation, the sample will soon undergo a catastrophic transition to the normal state. In fact, for the sample shown in Fig. 6, this catastrophy occurs whenever the total power dissipation in the sample reaches 1.1 mW. This critical power level depends also on the rate with which α is increased. When α is increased faster, the sample goes normal at a lower power level. This is no doubt caused by locally excessive values of α, as is the case with the flux jumps observed in tube experiments.

Thus, the critical value of α that can be reached in voltage measurements, which we designate by α_p, is limited by the power dissipation in the sample. Structural constants and thermal conductivity of the material as well as the cooling condition will enter into the determination of α_p. In the sample shown in Fig. 9, below T_λ the critical power level increases by a factor of 15 because of the better cooling condition. Even if all of these factors are held constant, however, α_p also depends on the value of J. This is clear from the dependence of P on α and J as given in (23). A larger value of α_p can be attained at a lower level of J, as shown in Fig. 8. This also explains why in tube experiments flux jumps are more frequent at the low field–high current region. In practical applications, this means that SIII materials will behave better at the low current–high field region than at the high current–low field region.

Also note that the average power expression (23) is meaningful only if a uniform condition is preserved through the entire length of the sample. Otherwise, α_p will be controlled by the weak spots in the sample. Some indications of this effect are evident if we compare the two samples shown in Figs. 8 and 9. Both samples shown here were taken from the same batch of wire and had been treated identically as far as practically possible. The comparison of $V(\alpha)$'s at 4.2°K indicates that the structural conditions are not the same for these two samples. Measurements were made on several more samples of varying lengths, but all taken from the same batch of wire. For any particular sample, however, $V(\alpha)$ could not be predicted with certainty on the basis of similar measurements made on other samples. This lead us to doubt the uniformity even among different sections of one sample. We therefore measured the voltages appearing across five different sections of a 250-cm-long wire sample (identical geometry to those shown in Figs. 8 and 9), by attaching to the sample six equally spaced voltage leads. $V(\alpha)$ obtained with this sample at 2.0°K is shown by curve (10) of Fig. 9. In this measurement, the voltage always appeared across one particular section. The voltages across the remaining four sections never rose above the noise level ($\sim 1\ \mu$V) throughout the entire range of $V(\alpha)$ observed.

The above test indicates that the resistive state as observed in the present experiments is controlled by a weak spot in the material. Flux creeps rapidly through this spot and instabilities leading to a catastrophy grow quickly. At present, very little is known about the exact nature of the weak spots and we are far from being able to control them. Consequently, the performance of a long length of wire cannot be predicted with certainty from measurements made on a small number of short samples, a fact that has been bothering those concerned with practical superconducting magnets. It is also obvious that such expressions as $\rho=V/lJ$ and $P=VJ/l$ containing the length of wire l, must be taken with some care. For example, the resistivity as given in Fig. 6 is certainly a gross underestimate.

In the analysis of the previous section, we tacitly assumed that the sample temperature T was close to the bath temperature T_B. Several observations justify this assumption. First, if T exceeds T_B appreciably, the great sensitivity of V on T would cause an increased slope in the $V(\alpha)$ curve just before the sample goes normal. This is, in fact, observed for curves (8) and (9) of Fig. 9, where the high thermal conduction of the helium bath below T_λ permits much higher power dissipation before the normal transition. Over most of the curves, however, there is no sudden change in slope, indicative that T must be close to T_B. Second, in Fig. 8 are shown curves taken with different values of J and hence at different power levels. However, they all properly coalesce to a single curve, indicating in each case that the sample temperature must be close to the 4.2°K bath. Figure 9 shows that this also occurs at the other temperatures. By relating the power dissipation in the equilibrium state to the conditions for thermal instabilities, we estimate that the region of a weak spot in our 3Nb-Zr sample is rather small. It could be as short in length as 10^{-3} cm. This may preclude any attempt to measure directly the local temperature of the sample.

VI. SUMMARY

In the present investigation, we have attempted to unify various phenomena observed in the resistive state of hard superconductors. Instrumental to this unification is the flux-creep theory. This theory assumes basically the Abrikosov mixed state, but the phenomena associated with transport currents are affected mainly by flux pinning. The central feature of the theory is that

flux pinned by physical irregularities present in the material can creep by thermal activation, the rate of creep being determined by the relative strength of pinning and magnetic pressure. The dissipative process associated with flux creep is intrinsically different from ohmic dissipation. Nevertheless, we may conveniently talk about electrical resistivity as such by equating power dissipation per unit volume to ρJ^2, as long as we confine this power into the region where the dissipation actually takes place.

Experimentally, the resistive state has been investigated by two methods: tube magnetization and resistance measurements. In both cases, the observations can be unified in terms of the Lorentz force parameter $\alpha=J(B+B_0)$. In tube magnetization, the internal field H' is measured as a function of the external field H (see Fig. 1) and α_c is determined from (3). If α is raised beyond α_c, flux creeps so fast that it quickly falls to α_c. Thus, α_c simply represents the value of α at which the rate of flux creep (12), or dH'/dt, falls below a certain level. For the tube geometries used in our experiments, this level corresponds, typically, to $\rho\sim10^{-13}$ Ω-cm [see (7)]. In time, both H' and α change linearly in $\ln t$, and ρ falls as $1/t$. ρ may fall by several orders of magnitude within a few hours, but the decrease in α during this period amounts to only a few percent. Therefore, the value of α_c determined by tube magnetization is not seriously affected by this transitory behavior. For the same reason, however, tube magnetization also restricts our observations to a narrow range of α near α_c. Specific verifications of the theory resulting from tube experiments are:

(1) At high fields ($B\gg B_0$), the observed temperature dependence of α_c (8) follows from the rate equation (12);

(2) The logarithmic decay as predicted by the theory [see (14)] has been verified. The dependence of decay rates on fields and temperature has not been fully tested, however;

(3) Experimental observations of discrete, stochastic pulses can be interpreted most naturally in terms of the flux-creep theory.

We tested the theory over a wider range of α variation by measuring resistance of *S*III samples. Voltages appearing across a sample were obtained as a function of externally supplied current J and transverse field H. We interpret this voltage as a manifestation of uncompensated emf arising from flux creep. We again find that at a given temperature the voltage so observed is a function of only $\alpha=J(H+B_0)$, B_0 being the same order of magnitude as found in tube experiments. $V(\alpha,T)$ follows (18), a form expected from the theory. These measurements gave rise to another critical value α_p, which is dictated by power dissipation in some local regions of the sample. When α reaches α_p, thermal conduction begins to lag power dissipation and thermal instabilities grow quickly from these regions, leading to a catastrophic transition to the normal state.

The summary presented above indicates that the flux-creep theory is very effective in unifying various phenomena associated with the resistive state of hard superconductors. In its present form, however, the theory is not adequate to account for: (a) the dependence of V on α, (b) the significance of B_0 and its temperature dependence, and (c) the "peak effect" observed in some material near the upper critical field.

ACKNOWLEDGMENTS

We are indebted to R. D. Dunlap for his collaboration in the experiments and to R. Epworth and J. Hasiak for their technical assistance. We are grateful to P. W. Anderson and T. H. Geballe for helpful discussions.

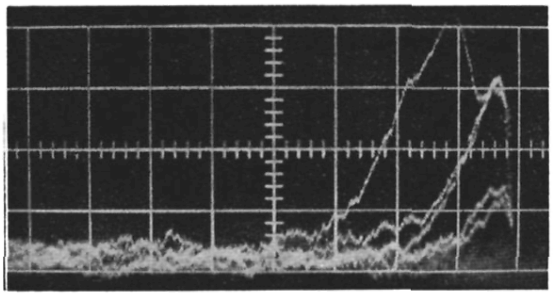

(a)

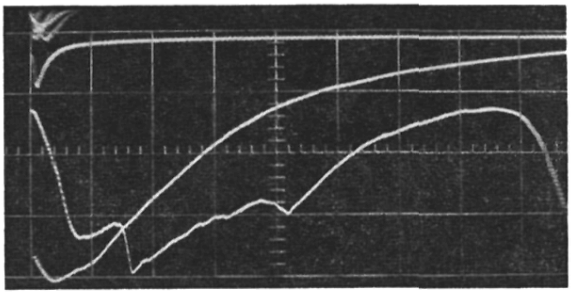

(b)

FIG. 5. Pulses observed in pickup coils of Fig. 1: (a) pulses observed in P_1 at the shielding region (20 μsec/div, 5μV/div); (b) pulses observed in P_2 at the circular region (200 μsec/div, 2 mV/div).